Reduced Graphene Oxide Embedded Polymeric Nanofiber Mats: An 'On-Demand' Photothermally-Triggered Antibiotic Release Platform

Ismail Altinbasak, Roxana Jijie, Alexandre Barras, Bianka Golba, Rana Sanyal, Julie Bouckaert, Djamel Drider, Rostyslav Bilyy, Tetiana Dumych, Solomiya Paryzhak, et al.

ACS APPLIED MATERIALS & INTERFACES

Research Article

www.acsami.org

Reduced Graphene-Oxide-Embedded Polymeric Nanofiber Mats: An "On-Demand" Photothermally Triggered Antibiotic Release Platform

Ismail Altinbasak,[†] Roxana Jijie,[§] Alexandre Barras,[§] Bianka Golba,[†] Rana Sanyal,[†,‡,∥] Julie Bouckaert,[⊥] Djamel Drider,[#] Rostyslav Bilyy,[▽] Tetiana Dumych,[▽] Solomiya Paryzhak,[▽] Volodymyr Vovk,[▽] Rabah Boukherroub,[§] Amitav Sanyal,*[,†,‡] and Sabine Szunerits*[,§]

[†]Department of Chemistry and [‡]Center for Life Sciences and Technologies, Bogazici University, Bebek, 34342 Istanbul, Turkey

[§]Université Lille, CNRS, Centrale Lille, ISEN, Université Valenciennes, UMR 8520 - IEMN, F-59000 Lille, France

[∥]RS Research Inc., Teknopark Istanbul, Pendik, 34912 Istanbul, Turkey

[⊥]Unité de Glycobiologie Structurale et Fonctionnelle (UGSF), UMR 8576 du CNRS et Université Lille, 50 Avenue de Halley, 59658 Villeneuve d'Ascq, France

[#]Institut Charles Viollette, Université de Lille1, EA 7394 Lille, France

[▽]Danylo Halytsky Lviv National Medical University, 79010 Lviv, Ukraine

Supporting Information

ABSTRACT: The steady increase in antimicrobial resistance in different pathogens requires the development of alternative treatment strategies next to the oral delivery of antibiotics. A photothermally activated platform based on reduced graphene oxide (rGO)-embedded polymeric nanofiber mats for on-demand release of antibiotics upon irradiation in the near-infrared is fabricated. Cross-linked hydrophilic nanofibers, obtained by electrospinning a mixture of poly(acrylic acid) (PAA) and rGO, show excellent stability in aqueous media. Importantly, these PAA@rGO nanofiber mats exhibit controlled photothermal heating upon irradiation at 980 nm. Nanofiber mats are efficiently loaded with antibiotics through simple immersion into corresponding antibiotics solutions. Whereas passive diffusion based release at room temperature is extremely low, photothermal activation results in increased release within few minutes, with release rates tunable through power density of the applied irradiation. The large difference over passive and active release, as well as the controlled turn-on of release allows regulation of the dosage of the antibiotics, as evidenced by the inhibition of planktonic bacteria growth. Treatment of superficial skin infections with the antibiotic-loaded nanofiber mats show efficient wound healing of the infected site. Facile fabrication and implementation of these photothermally active nanofiber mats makes this novel platform adaptable for on-demand delivery of various therapeutic agents.

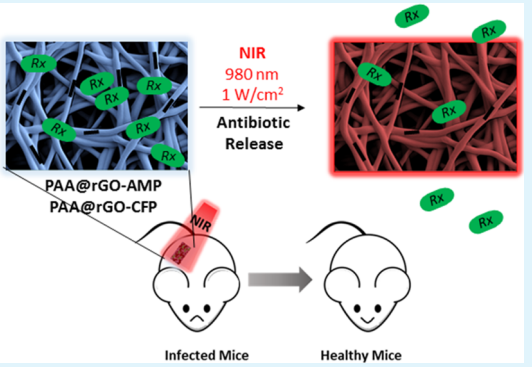

KEYWORDS: *electrospinning, nanofibers, reduced graphene oxide, antibiotic release, photothermal effect*

INTRODUCTION

One of the challenges frequently encountered in traditional methods of drug delivery relates to poor control over proper dosage of therapeutic agent.[1−3] Maintaining the drug concentration within a particular therapeutic window and below toxic concentrations is challenging, and lack of efficient treatment can lead to severe side effects, along with the development of drug resistance in cells and pathogens. These problems have fostered the development of different approaches that enable the controlled release of a precisely defined amount of drug, but allow in addition the release of the therapeutic dose on demand, upon the application of an external trigger rather than by passively driven diffusion processes. In the last decade, several delivery systems have been fabricated to deliver drug locally by controlling release kinetics through utilization of various types of stimuli, either external or intrinsic to the disease site.[4,5] The capability to tune the physicochemical properties of polymeric nanostructures as well as other advantages such as their stability in vitro and in vivo conditions and good biocompatibility has laid the foundation for the emergence of a large number of polymeric nanosystems for controlled drug release.[6−9]

Received: August 27, 2018
Accepted: October 30, 2018
Published: October 30, 2018

DOI: 10.1021/acsami.8b14784
ACS Appl. Mater. Interfaces XXXX, XXX, XXX−XXX

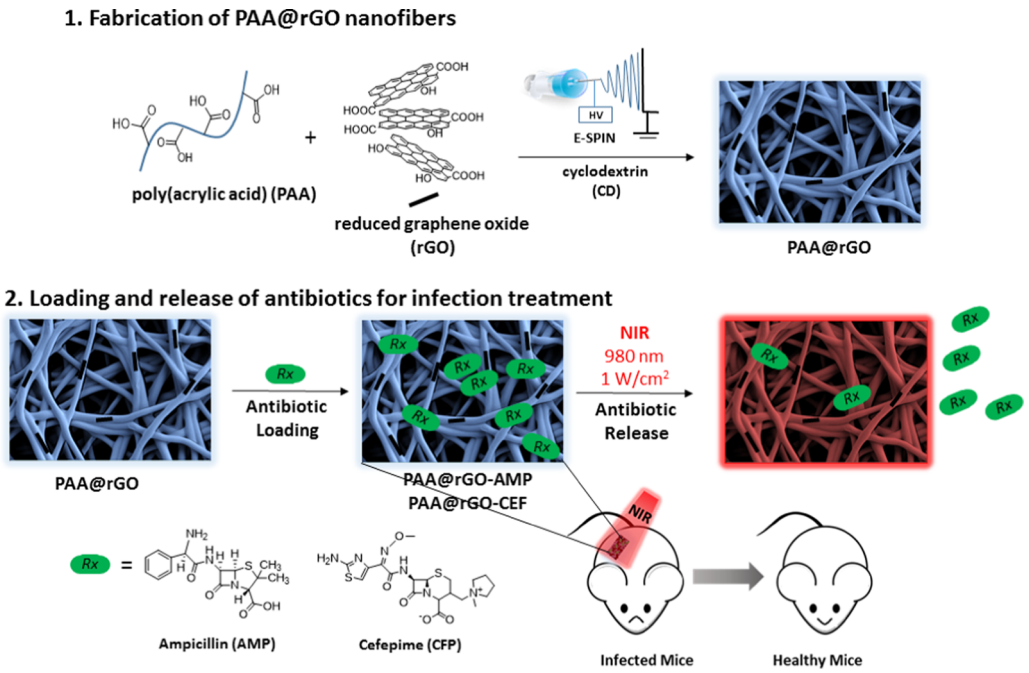

Figure 1. Illustration of the fabrication of antibiotic-loaded PAA@rGO nanofibers: (1) electrospinning of rGO-loaded PAA nanofiber mats followed by (2) loading with different antibiotics and photothermal-triggered antibiotic release.

Over the past decades, there is considerable evidence of the benefits polymeric materials as antibiotic delivery platform.[10−12] Polymeric materials have shown to solve problems related to the solubility of hydrophobic antibiotics, as well as provide a protective coating against environmental degradation and deactivation through the body's clearing mechanisms. The structures proposed range from discrete soluble polymers conjugated with antibiotics[13] to materials where polymers are chemically or physically assembled in the form of hydrogels,[14−17] micelles,[18] nanogels,[19] nanoparticles,[20] and nanofibers.[21] Polymeric nanoparticles are well suited for addressing bacterial infections inside the body as the nanometric size of antibiotic-loaded nanoparticles enables efficient penetration through the mucus layer around bacteria biofilms, thus increasing the local concentration of antibiotic in the biofilm.[1] On the other hand, antibiotic-loaded bandages, foams, and dressings are preferential for external applications such for the management of chronic wounds.[22,23] In this regard, antibiotic-loaded nonwoven fibrous materials obtained using polymeric nanofibers could be ideal candidates for wound infection treatment, as they can be directly fabricated in the form of ready-to-apply materials. One of the most commonly encountered challenge in wound healing is infection. Next to iodine- or silver-ion-containing dressing, antibiotic ointments are regularly used to prevent wound infection.[24] In the case of antibiotic ointments, discomfort caused to the patient, along with the chances of developing resistance to antibiotics and contact dermatitis, has put their efficiency into question.[25]

One attractive alternative as a wound-healing material and a protective scaffold after surgical procedures favoring site-specific therapy by increasing the local antibiotic concentration might be the use of antibacterial-loaded nanofiber mats. These polymeric scaffolds are engineered via a polymer-processing technique called electrospinning, which allows usage of a variety of polymers with different chemical composition and morphology.[26−28] This enables to select the most appropriate material for the intended application and enables tailoring of drug release profiles.[29] Hadjiargyrou and co-workers demonstrated the incorporation of hydrophilic antibiotics (mefoxin and cefoxitin) and their release in a sustained manner from poly(lactide-co-glycolide) nanofiber-based scaffolds obtained using electrospinning, without any compromise in their bioactivity and structure.[30] A passive diffusion release of about 70% of loaded cefoxitin was observed in the first hour, and the rest of the loaded antibiotic was released over 1 week. Although the antibiotic that was released from these nanofibers was effective in inhibiting *Staphylococcus aureus* growth (>90%), burst release is an undesirable feature. To achieve an antibiotic release at the constant rate over a prolonged time period, stimuli-responsive nanofibers have been designed, mainly using pH-based triggers.[31,32] For example, ciprofloxacin-loaded pH-responsive electrospun nanofibers fabricated from a copolymer of vinyl benzoic acid and vinylbenzyltrimethylammonium chloride, as reported by Uyar and co-workers, undergo enhanced drug release at pH 5.8. Although external modulation of pH is nontrivial, modulation of temperature is unique, as it can be considered to be either internal stimuli as some infections are naturally at elevated temperature, or to be external through the application or generation of heat in the nanostructure. In the case of polymers, a temperature change can result in rapid swelling of its structures, leading to high volume alterations and thus inducing enhanced drug release.[7] Some photothermal active nanofibers formed through the incorporation of gold nanostructures,[33−35] carbon nanotubes,[36,37] carbon nanoparticles,[38] or more recently Cu_2S[39] have been described. We have shown lately the interest in reduced graphene-oxide (rGO)-loaded hydrogels for photothermal-initiated insulin release.[40]

Interestingly, although reports of graphene oxide (GO) and rGO-containing nanofibers have emerged in recent years,[41−44] only one report used the photothermal properties of the resulting nanocomposite,[45] and showed photothermal eradication of captured cancer cells. The photothermally triggered

DOI: 10.1021/acsami.8b14784
ACS Appl. Mater. Interfaces XXXX, XXX, XXX−XXX

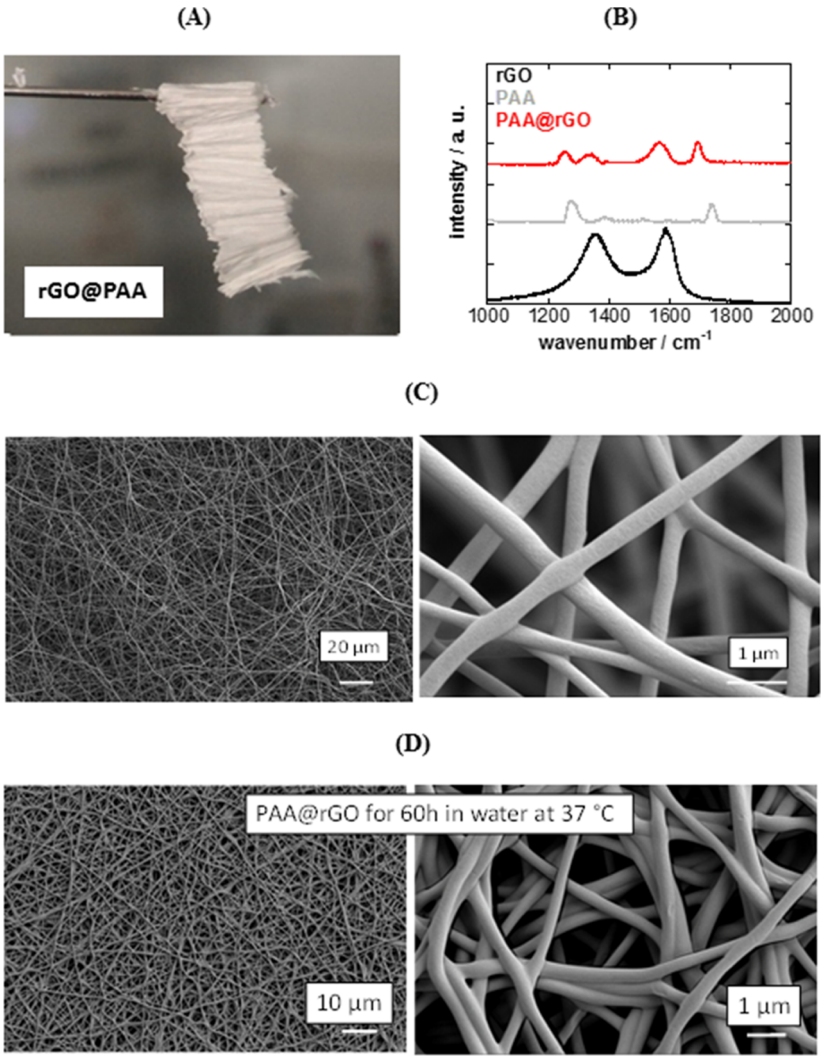

Figure 2. Characterization rGO-loaded PAA nanofiber mats formed by electrospinning: (A) photograph of electrospun PAA@rGO; (B) Raman spectra of rGO (black), PAA (gray), and PAA@GO (red); (C) scanning electron microscopy (SEM) images of fabricated PAA@rGO nanofiber mats at different scales; and (D) stability of β-cyclodextrin cross-linked PAA@rGO nanofibers in water at 37 °C for 60 h.

release of antibiotics from rGO-containing nanofibers and its use for the treatment of infections has not been explored until now. Herein, we disclose rGO-containing poly(acrylic acid) (PAA) based nanofiber mats (PAA@rGO) for the loading of different antibiotics due to their swelling and noncovalent interaction with rGO, as well as demonstrate controlled and on-demand release promoted by near-infrared photothermal heating (Figure 1). To allow facile diffusion of antibiotics under aqueous environment into nanostructures, we opted for the formation of rGO-loaded hydrophilic nanofibers by electrospinning PAA in the presence of cyclodextrin as a cross-linker. These nanofiber mats showed controlled photothermal heating ability, with the temperature reaching 67 ± 2 °C using a light source of 980 nm and 1 W cm^{-1} power density. The PAA@rGO nanomats showed high loading capability for ampicillin (AMP) and cefepime (CFP) with minimal passive antibiotic release. Ampicillin, part of the aminopenicillin family, was chosen for its favorable structure (aromatic ring together with the presence of amine and acid functional groups), enabling ampicillin to interact with rGO through electrostatic and π-stacking interactions (Figure 1). The same is true for cefepime (CFP), an antibiotic belonging to the class of cephalosporin commonly applied for the treatment of bacterial conditions such as pneumonia, kidney, urinal, as well as skin infections. This antibiotic works by simply stopping the growth of bacteria.[46,47] Enhanced drug release was achieved under irradiation of the antibiotic-loaded PAA@rGO nanofiber mats with near-infrared light at 980 nm, where the antibiotic release rate can be tuned upon using different power densities. In vitro antibacterial assay demonstrates clearly that the released antibiotics did not lose their biological activity to inhibit growth of pathogens. The nanofiber platform could be reloaded with antibiotic and release was achieved in a controlled fashion, thus demonstrating recyclability of the platform. Furthermore, through in vivo studies on *S. aureus* infected Balb/c mice, the antibiotic-loaded PAA@rGO nanofiber mats demonstrated excellent wound-healing capability, making them viable candidates for clinical applications.

EXPERIMENTAL SECTION

Materials. Poly(acrylic acid) (PAA, M_n = 450 000 g mol^{-1}), hydrazine, β-cyclodextrin, phosphate-buffered saline (PBS, pH 7.4) and cefepime were purchased from Sigma-Aldrich. Ampicillin (AMP)

DOI: 10.1021/acsami.8b14784
ACS Appl. Mater. Interfaces XXXX, XXX, XXX−XXX

was obtained from Fisher BioReagents (BP1760-25). Graphene oxide (GO) in powder form was purchased from Graphenea (Spain).

Characterizations and Photothermal Setup. Details of characterization techniques and instrumental details for photothermal setup employed in this study can be found in the Supplementary Information.

Fabrication of rGO-Loaded PAA Nanofiber (PAA@rGO). A GO precursor was chemically reduced to reduced graphene oxide (rGO) using hydrazine according to a procedure previously reported by us.[40,48] Briefly, GO aqueous suspension (5 mL, 0.5 mg mL^{-1}) was treated with hydrazine (0.50 mL, 32.1 mM) at 100 °C for 24 h. After this time, the reduced GO gradually precipitates. Filtration through a poly(vinylidene difluoride) membrane (0.45 μm pore size) is used to collect the product. Obtained residue is washed with copious amounts of water (5 × 20 mL) and methanol (5 × 20 mL). Finally, the product is dried in an oven for 18 h at 100 °C. Thereafter, to rGO aqueous suspension (1.2 mL, 2.5 mg mL^{-1}) was added PAA (100 mg) and β-cyclodextrin (20 mg) and the resulting mixture was stirred for 24 h at room temperature. This corresponds to rGO (2.4 wt %), PAA (81.4 wt %), and β-cyclodextrin (16.2 wt %). Clear polymer solution of PAA, β-cyclodextrin, and rGO was electrospun using a 1 mL syringe fitted with a 14-gauge blunt needle at the rate of 0.005 mL min^{-1} with 15 kW. The distance was kept at 15 cm during the electrospinning process. Resulting electrospun fibers were cross-linked under vacuum at 140 °C for 30 min.

Loading of Antibiotics onto Nanofibers. Antibiotics loading into the nanofibers was achieved by immersing the nanofiber mat (4 mg) into the aqueous solution of ampicillin (80−400 μg mL^{-1}) or cefepime (80−400 μg mL^{-1}) and shaking (150 rpm) at 4 °C for 72 h. The concentration of ampicillin and cefepime loaded into the nanofibers was determined from the absorption intensity of the AMP and cefepime remaining in the solution using high-performance liquid chromatogram (HPLC). Ampicillin and cefepime calibration curves were obtained using a series of antibiotic-containing solutions (1−100 μg mL^{-1}) (Figure S2).

Photothermal-Triggered Antibiotics Release. Antibiotic release was assessed in phosphate-buffered saline (PBS) (1 mL, pH 7.4) through direct irradiation of the nanofibers using a continuous wave laser at 980 nm at varying power densities (1−2 W cm^{-2}) for several minutes. The amount of antibiotics released was determined from HPLC results of the solution collected after irradiation using previously established calibrations curves (Figure S2). Control experiments were carried out in an environmentally controlled cabin at 37 °C, and the samples were gently shaken during incubation.

Wound Healing and Histology. Full details of the study can be found in the Supplementary Information. Briefly, 6−8-week-old male Balb/c mice were used for this study. The superficial skin damaged infection model was performed as described by us previously[49] with some modifications. After removing the fur, a plaster was applied to the mouse skin (1 cm^2) several times to remove the superficial epidermis. The skin damaged was visible and characterized by reddening and glistening but no regular bleeding. Then, 10 μL of *S. aureus* bacterial cells (4 × 10^7 cfu mL^{-1}) were applied to the skin and allowed to dry for 10 min. Superficial skin infection established after 24 h and PAA- or cefepime-loaded PAA@rGO nanofiber mats were applied to the skin of the anesthetized mice. Untreated mice were used as control. The mat was irradiated for 10 min with a near-infrared light-emitting diode (LED) array (6 × 6 mm^2 in size, 8 W, 2A, 940 nm), previously shown to be a safe condition for animals.[49] The temperature was monitored by an infrared camera (Thermovision A40). Mice were photographed and images were processed with ImageJ software to detect erythema, and its area before and after a 24 h treatment was evaluated. After 24 h, the mice were sacrificed and the skin was removed and subjected to histological analysis.

RESULTS AND DISCUSSIONS

Fabrication and Characterization of rGO-Containing Nanofibers. First, rGO-containing PAA nanofibers were obtained through electrospinning of an aqueous dispersion of rGO (2.4 wt %), PAA (81.4 wt %), and β-cyclodextrin (16.2 wt %) as a cross-linker (Figure 1). Upon electrospinning, a free standing mat of electrospun fibers is obtained (Figure 2A). Raman spectra of PAA and PAA@rGO were recorded to confirm the incorporation of rGO into the nanofibers (Figure 2B). Raman analysis revealed the presence of the expected bands at ≈1350 cm^{-1} (D-band) and ≈1580 cm^{-1} (G-band) due to the defects and disorders, and the graphitized structure of rGO, respectively (Figure 2B). The I_D/I_G intensity ratio was found to be 0.93 for rGO. The PAA fibers did show a Raman band at 1728 cm^{-1} assigned to C═O functional groups, whereas the bands at 1235 and 1285 cm^{-1} are ascribed to $-CH_2-$ bonds.[50] In the case of PAA@rGO, the bands of rGO are identifiable in the Raman spectrum. Additionally, Fourier transform infrared (FTIR) and X-ray photoelectron spectroscopy (XPS) spectra of PAA@rGO were obtained, where the FTIR analysis did not provide any information about rGO incorporation due to its low amount, but the presence of delocalized π-electrons was evident in the XPS spectra (C 1s scan) (Figure S3).

To ensure long-term stability in the aqueous media of the hydrophobic PAA@rGO nanofibers, the fibers were cross-linked to prevent their dissolution. As reported earlier, β-cyclodextrin, a molecule containing multiple hydroxyl groups can be efficiently used to cross-link the PAA polymer upon heat treatment under vacuum for 30 min.[51] The morphology of the resulting cross-linked PAA@rGO nanofibers was probed using scanning electron microscopy (SEM). Figure 2C shows the formation of dense mats of interwoven nanofibers 400 ± 150 nm in diameter. Furthermore, the integration of rGO did not alter the morphology of the nanofibers (see the Supporting Information, Figure S1). The stability of the cross-linked PAA@rGO nanofibers was validated by immersing them into aqueous solutions for several days at 37 °C. From the SEM images in Figure 2D, it is evident that the cross-linked PAA@rGO nanofibers preserve their nanostructures and no dissolution of the fiber networks occurs even after immersion for days.

After fabrication, the photothermal properties of the PAA@rGO nanofiber mats were explored (Figure 3A). Whereas PAA displayed only a negligible photothermal heating, direct irradiation of PAA@rGO (4 mg immersed in 1 mL PBS) with a continuous wave laser at 980 nm (1 W cm^{-2}) for 5 min results in a surface temperature of about 67 ± 2 °C. Even decreasing the laser power density to 0.5 W cm^{-2} showed a

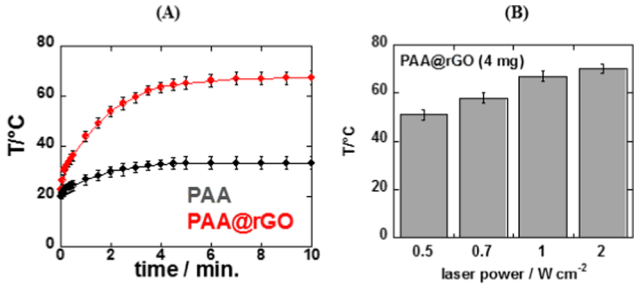

Figure 3. Photothermal properties of cross-linked PAA@rGO: (A) photothermal heating curves of PAA (gray) and PAA@rGO (red) nanofiber patches (4 mg) immersed in PBS (0.1 M, pH 7.4) and irradiated at 980 nm (1 W cm^{-2}) for 10 min and (B) temperature profile of PAA@rGO nanofiber mats upon 10 min irradiation at varying power densities.

DOI: 10.1021/acsami.8b14784
ACS Appl. Mater. Interfaces XXXX, XXX, XXX−XXX

rapid increase in the surface temperature of PAA@rGO nanofibers, reaching saturation at approximately 51 ± 2 °C within 5 min in a wet environment. No melting of nanofibers occurred under the used conditions, thus preserving the structural integrity of the fibrous mats. Thus, with modulation of laser power density, these nanofiber mats exhibited controlled photothermal heating ability within a temperature range from 20 to 67 ± 2 °C.

Loading and Release of Antibiotics into Nanofibers. Integration of antibiotics into the cross-linked PAA@rGO nanofiber mats was achieved by simply immersing the nanofibers into the aqueous solution of ampicillin or cefepime in water at 4 °C for 72 h. Both antibiotics contain aromatic structures together with amino and carboxylic acid functional groups, thus promoting their interaction with rGO through $\pi-\pi$ stacking and/or electrostatic interactions. The loading capacity of PAA@rGO nanofibers for AMP and cefepime was determined from the amount of the antibiotic in the solution before and after loading using HPLC. The loading capacity of PAA@rGO for ampicillin and cefepime is comparable as seen in Figure 4A. Using the solution concentration of 400 μg mL^{-1}

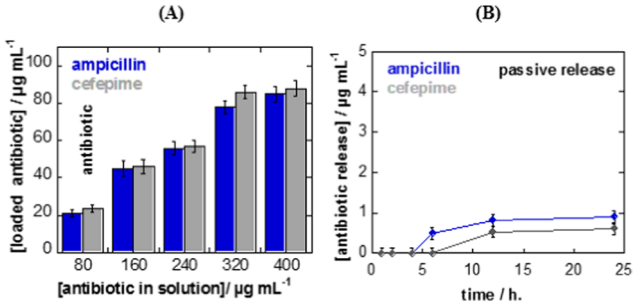

Figure 4. (A) Loading capacity of PAA@rGO nanofiber mats (4 mg) with ampicillin and cefepime upon incubation for 24 h into PBS (0.1 M, pH 7.4) under shaking at different drug concentration. (B) Passive release from antibiotic-loaded cross-linked PAA@rGO nanofibers when immersed in 0.1 M PBS (pH 7.4) for 24 h at 37 °C.

of the antibiotics resulted in the loading of about 85 ± 3 μg mL^{-1} (21%) and 89 ± 3 μg mL^{-1} (22%) for ampicillin and cefepime, respectively. Ampicillin has a pK_a ≈ 4−5 (COOH) and pKa ≈ 9 (NH_2), making it zwitterionic at physiological pH. A fair amount of the amine groups are positively ionized at physiological pH and this promotes their interaction with the PAA@rGO nanofiber mats (pK_a ≈ 4.5).[52] The quaternary ammonium group of the *N*-methylpyrrolidine groups in cefepime (Figure 1) makes the drug positively charged and results in interaction with the ionized carboxylic acid groups in PAA and negatively charged rGO that has a ζ-potential of −50 ± 2 mV. Due to their hydrophilic nature, it can be expected that the nanofibers swell in aqueous media and thus load the antibiotics efficiently. Remarkably, the passive release from the antibiotic-loaded PAA@rGO nanofibers, PAA@rGO−AMP, and PAA@rGO−CFP, was found to be negligible. For the first 5 h, the amount of antibiotic release was below the detection limit of the HPLC analysis. After 24 h incubation in PBS (0.1 M, pH 7.4) about 0.8 ± 0.1% was released via passive diffusion (Figure 4B).

Encouraged by the excellent stability of the PAA@rGO to retain the loaded antibiotics, we explored the photothermal properties of the PAA@rGO nanofiber mat to trigger the drug release. Figure 5A shows the release profiles for ampicillin as

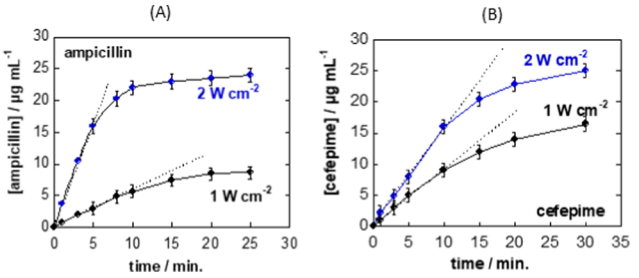

Figure 5. Photothermal-triggered antibiotics' release for PAA@rGO nanofibers: (A) release profile of ampicillin from a PAA@rGO nanofibers loaded with ampicillin (25 μg mL^{-1}) when activated at 980 nm at 2 and 1 W cm^{-2} and (B) release profile of cefepime from PAA@rGO nanofibers loaded with cefepime (25 μg mL^{-1}) when activated at 980 nm at 2 and 1 W cm^{-2}.

well as cefepime upon irradiating PAA@rGO nanofibers loaded with ampicillin (25 μg mL^{-1}) and cefepime (25 μg mL^{-1}) with NIR light. Using a laser power density of 2 W cm^{-2} results in an almost complete release of ampicillin (24 μg mL^{-1}; ≈96% of loaded ampicillin) with a release rate of 3.2 μg mL^{-1} min^{-1}, which can be lowered to 0.5 μg mL^{-1} min^{-1} using a phototrigger of 1 W cm^{-2}. The released ampicillin concentrations are much larger than the minimum inhibitory concentration (MIC) value of ampicillin for Gram-negative *Escherichia coli* K12 (Table 1). Ampicillin shows no activity for *S. aureus* and *Staphylococcus epidermidis*.

Table 1. Minimum Inhibitory Concentrations of Ampicillin and Cefepime for Different Bacteria Strains

antibiotic	MIC$_{50}$/μg mL^{-1} (*E. coli* K12)	MIC$_{50}$/μg mL^{-1} (*S. aureus* ATCC 25923)	MIC$_{50}$/μg mL^{-1} (*S. epidermidis*)
ampicillin	4.9 ± 0.5		
cefepime	1.1 ± 0.3	4.1 ± 0.8	10 ± 1.8

In the case of cefepime-loaded nanofiber mats, photothermal activation of the fibers with 2 W cm^{-2} leads to a complete release of the entrapped antibiotic (25 μg mL^{-1}) in a time frame of ≈25 min, with a release rate of 1.36 μg mL^{-1} min^{-1} for cefepime for the first 10 min. The release rate can be tuned upon using a lower power density: using a laser power of 1 W cm^{-2}, the release rate of cefepime decreased to 0.91 μg mL^{-1} min^{-1}. Importantly, no burst release was observed in any of these examples and the maximal amount released is about twice of the MIC value for cefepime for *S. epidermidis* and several times larger than the MIC value for cefepime for *E. coli* K12 and *S. aureus* ATCC 25923 (Table 1).

Antibacterial Activity under Passive and Active Release. Although ampicillin has sufficient stability in the dry state, it is only short lived in a solution. Following photothermal-triggered ampicillin release, their antibiotic efficiency was assessed by determining the titer of viable bacteria able to grow. Figure 6A shows the change in OD$_{600}$ values upon *E. coli* K12 incubation with different ampicillin-released samples at 1 W cm^{-2}. In agreement with the photothermal release profile (Figure 5A), about 2.5 μg mL^{-1} of ampicillin are released in the first minute, below the MIC$_{50}$ value, whereas 6.8 μg mL^{-1} ampicillin (above the MIC$_{50}$ value) was released after 3 min, resulting in the inhibition of *E. coli* growth. This underlines the fact that the photothermal-triggered ampicillin release does not effect the biological activity of the antibiotic.

DOI: 10.1021/acsami.8b14784
ACS Appl. Mater. Interfaces XXXX, XXX, XXX−XXX

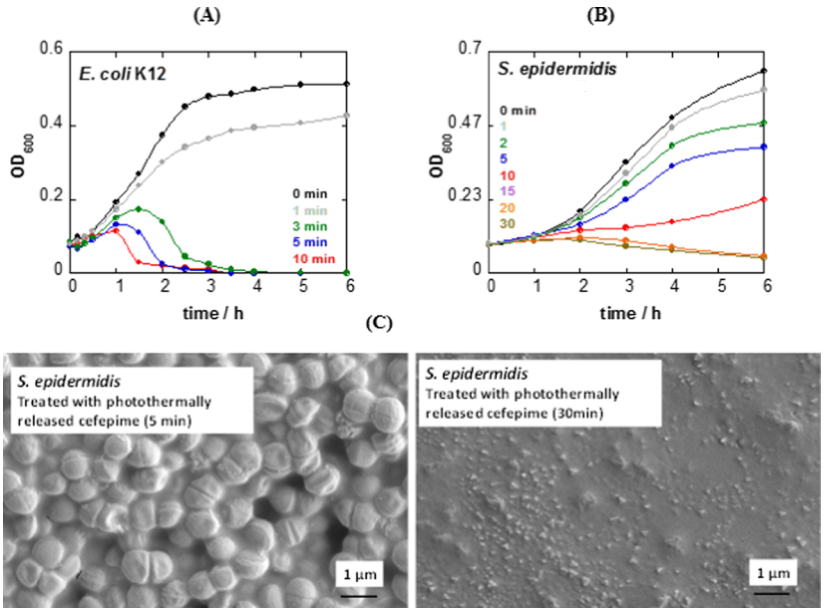

Figure 6. (A) Planktonic growth of *E. coli* K12 (1×10^8 cfu mL^{-1}) (A) without ampicillin (black, $t = 0$) and when treated with ampicillin released photothermally from PAA@rGO nanofiber mats at different time intervals corresponding to Figure 5A. (B) Planktonic growth of *S. epidermis* without cefepime (black, $t = 0$) and when treated with cefepime released photothermally from PAA@rGO nanofiber mats at different time intervals corresponding to Figure 5B. (C) SEM images of *S. epidermidis* treated with cefepime photothermally released from PAA@rGO nanofiber mats for 5 and 30 min.

Whereas ampicillin is only effective toward Gram-negative *E. coli* K12, cefepime is active for Gram-negative and Gram-positive strains, with a higher MIC for *S. epidermidis* strain. *S. epidermidis* are known to be one of the most frequently encountered skin-colonizing bacteria and the predominant causes of nosocomial and community-associated skin infections. As expected, cefepime doses proved to be active against *S. epidermidis*. Cefepime released from cefepime-loaded nanofibers shows a release-dependent killing effect on *S. epidermidis* in accordance with the release profile determined in Figure 5B. Figure 6C shows the SEM images of *S. epidermidis* treated with photothermally released cefepime. Whereas the amount of cefepime is below the MIC value after 5 min and does not effect in any way the *S. epidermidis* growth, the pathogen is completely destroyed above the MIC value (corresponding to times >10 min). This indicates that the developed approach can be easily adapted for any desired antibiotic to eliminate a particular bacterial strain.

In addition to sustained antibiotic release, an important feature of any drug-release system is its reusability. Reloading of PAA@rGO with ampicillin or cefepime, as well as photothermally induced release could be attained with the similar efficiency over several cycles (Figure 7). Apart from just the possibility of reuse, the multiple loadings and release of antibiotics also demonstrate that the extent of upload and release is highly reproducible for these nanofibrous mats.

Infectious Wound-Healing Studies Using rGO Nanofibers. There are different experimental models of skin infections that are caused by *S. aureus*.[53,54] In our research, the bacteria were directly applied on the previously damaged skin. The tape-stripping approach, one of the most common models for the generation of superficial skin infection in mice,[55] was used here, as it allows to establish superficial infections in the epidermis, as well as the upper layer of the dermis. We monitored the skin infection progress in three animal groups: those treated with skin application of cefepime-

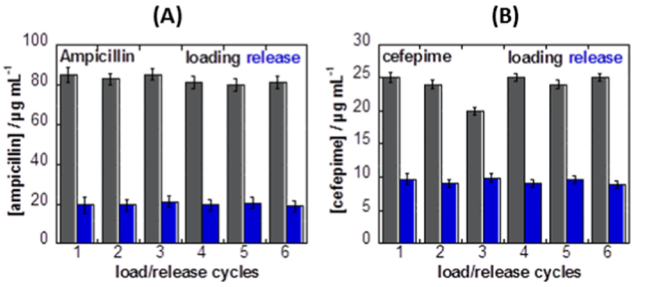

Figure 7. (A) Loading of ampicillin (85 μg mL^{-1}) and the amount of photothermally released ampicillin after 10 min laser irradiation (1 W cm^{-1}). (B) Loading of cefepime (25 μg mL^{-1}) and release of cefepime when activated at 980 nm at 2 W cm^{-2}.

loaded either PAA (PAA-CFP) or PAA@rGO (PAA@rGO-CFP) nanofiber mats and untreated mice (controls). The treatment in all groups started 24 h following the infection induction. Figure 8 displays images of the noninfected- and infected-wound groups untreated and treated with antibiotic-loaded nanofiber mats 48 h after infection initiation. The dressing (white arrows) was applied tightly to the wound area. The untreated areas and those treated with cefepime-loaded PAA nanofiber mats (PAA-CFP) and light activated for 10 min to release the antibiotics revealed inflammation and areas with abundant edema, erythema, and bacterial infiltration/pus. Blood vascularization and bacterial infiltration are in addition detected in the untreated groups and cefepime-loaded PAA fiber mats without embedded rGO (Figure 8B). This is in contrast to cefepime-loaded PAA@rGO mats, wherein the photothermal treatment prevented the bacteria from spreading (Figure 8A). Infected layers after 10 min illumination with a LED array through the antibiotic-loaded PAA@rGO nanofiber mats (PAA@rGO-CFP) show signs of resolution of inflammation (Figure 8A) and reduced blood vascularization and bacterial infiltration (Figure 8B). No damage to skin was

DOI: 10.1021/acsami.8b14784
ACS Appl. Mater. Interfaces XXXX, XXX, XXX−XXX

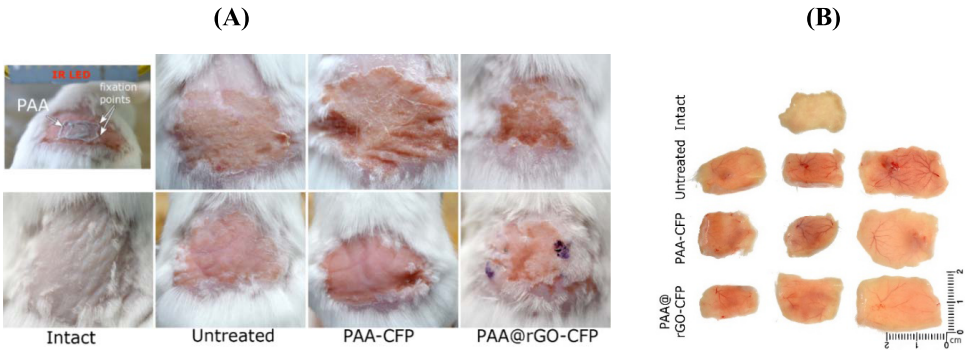

Figure 8. (A) Photographs of wound scars 24 h after treatment (980 nm, 1 W cm^{-2}) for 10 min with cefepime-loaded nanofibers mats (PAA-CFP; PAA@rGO-CFP). Negative control—intact skin; positive control—infected untreated skin. Insert at top left demonstrates the setup for animal treatment. (B) Photographs of intact mouse skin and three representative skin samples after 48 h of infection under different treatment conditions.

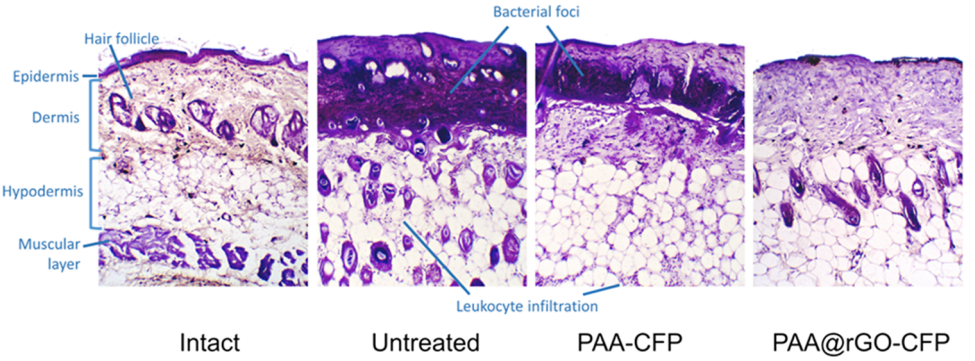

Figure 9. Histological examination of skin wound healing 48 h after the infection. Sections of skin tissues with Gram staining. Intact mouse skin; untreated skin (after infection); and photothermally treated infected skin part of the wound (PAA-CFP and PAA@rGO-CFP).

observed with LED illumination of the PAA@rGO nanofiber patch during the in vivo experiments, as the skin surface temperature was kept maximal at 52 °C. ~~This is opposed to~~ skin heating up to 67 °C ~~when tissue~~ damage ~~could be~~ observed ~~in~~ meat samples (Figure S4).

Histological section of a representative skin specimen (harvested at day 2 postinfection) after Gram staining (Figure 9) showed that *S. aureus* was superficially localized in the epidermis and penetrated the dermis layers of untreated and PAA-CFP skin samples. In addition, ~~the~~ leukocytic infiltration was abundant in the deep layer of hypodermis, indicating abundant bacterial presence. However, the infected wound irradiated through the antibiotic-loaded PAA@rGO patch for 10 min indicated active wound healing without marks of inflammation and bacterial foci. ~~Epidermis~~ revealed signs of active regeneration. Thus, it could be concluded that the topical application of PAA@rGO-CFP mats for photothermal therapy exhibited the best wound-healing capability among those tested.

CONCLUSIONS

In summary, a novel nanofiber-based platform for "on-demand" release of antibiotics is fabricated using rGO-containing polymeric nanofibers. The rGO-embedded hydrophilic nanofibers obtained using solution electrospinning are loaded with two different antibiotics, namely, ampicillin and cefepime. Although negligible release of antibiotic is observed under physiological conditions, exposure to NIR irradiation leads to release amounts sufficient to kill Gram-positive and Gram-negative bacteria alike. A clear correlation between the NIR-triggered antibiotic release and bactericidal activity is observed. It can be anticipated that the facile fabrication and modular nature of the construct reported here provides a platform that can be adapted for on-demand delivery of various drugs for combating different diseases. Although only two specific antibiotics were chosen in this study, the platform is amenable to loading of other antibiotics, either solo or in combination to combat a plethora of bacterial infections.

ASSOCIATED CONTENT

Supporting Information

The Supporting Information is available free of charge on the ACS Publications website at DOI: 10.1021/acsami.8b14784.

SEM images of fabricated PAA nanofiber mats at different scales, HPLC plot, and calibration curves of antibiotic release studies, FTIR and XPS of PAA@rGO and images of skin samples treated with NIR irradiation (PDF)

AUTHOR INFORMATION

Corresponding Authors

*E-mail: amitav.sanyal@boun.edu.tr. Tel: +902123597613 (A.S.).

*E-mail: sabine.szunerits@univ-lille.fr. Tel: +33 (0)3 62 53 17 25 (S.S.).

ORCID

Rana Sanyal: 0000-0003-4803-5811

Julie Bouckaert: 0000-0001-8112-1442

Rostyslav Bilyy: 0000-0002-2344-1349

Rabah Boukherroub: 0000-0002-9795-9888

DOI: 10.1021/acsami.8b14784
ACS Appl. Mater. Interfaces XXXX, XXX, XXX−XXX

Amitav Sanyal: 0000-0001-5122-8329
Sabine Szunerits: 0000-0002-1567-4943

Author Contributions

The manuscript was written through contributions of all the authors.

Funding

This project has received funding from the European Union's Horizon 2020 Research and Innovation Staff Exchange (RISE) Marie Skłodowska-Curie Actions under grant agreement no. 690836.

Notes

The authors declare no competing financial interest.

■ ACKNOWLEDGMENTS

The Centre National de la Recherche Scientifique (CNRS), the University Lille 1, the Hauts-de-France region, the CPER "Photonics for Society", the Agence Nationale de la Recherche (ANR), and the EU union through FLAG-ERA JTC 2015-Graphtivity are acknowledged for financial support.

■ REFERENCES

(1) GuhaSarkar, S.; Bannerjee, R. Intravesical drug delivery: Challenges, current status, opportunities and novel strategies. *J. Controlled Release* **2010**, *148*, 147−159.
(2) Liu, D.; Yang, F.; Xiong, F.; Gu, N. The Smart Drug Delivery System and Its Clinical Potential. *Theranostics* **2016**, *6*, 1306−1323.
(3) Tiwari, G.; Tiwari, R.; Sriwastawa, B.; Bhati, L.; Pandey, S.; Pandey, P.; Bannerjee, S. K. Drug Delivery Systems: An Updated Review. *Int. J. Pharm. Invest.* **2012**, *2*, 2−11.
(4) Szunerits, S.; Teodorescu, F.; Boukherroub, R. Electrochemically Triggered Release of Drugs. *Eur. Polym. J.* **2016**, *83*, 467−477.
(5) Ganta, S.; Devalapally, H.; Shahiwala, A.; Mansoor, A. A Review of Stimuli-Responsive Nanocarriers for Drug and Gene Delivery. *J. Controlled Release* **2008**, *126*, 187−204.
(6) Kamaly, N.; Yameen, B.; Wu, J.; Farokhzad, O. C. Degradable Controlled-Release Polymers and Polymeric Nanoparticles: Mechanisms of Controlling Drug Release. *Chem. Rev.* **2016**, *116*, 2602−2663.
(7) Karimi, M.; Zangabad, P. S.; Ghasemi, A.; Amiri, M.; Bahrami, M.; Malekzad, H.; Asl, H. G.; Zahra Mahdieh, Z.; Mahnaz Bozorgomid, M.; Amir Ghasemi, A.; Rahmani Taji Boyuk, M. R.; Hamblin, M. R. Temperature-Responsive Smart Nanocarriers for Delivery Of Therapeutic Agents: Applications and Recent Advances. *ACS Appl. Mater. Interfaces* **2016**, *8*, 21107−21133.
(8) Li, Y.; Liu, G.; Waqng, X.; Hu, J.; Liu, S. Enzyme-Responsive Polymeric Vesicles for Bacterial-Strain-Selective Delivery of Antimicrobial Agents. *Angew. Chem., Int. Ed.* **2016**, *55*, 1760−1764.
(9) Weng, L.; Xie, J. Smart Electrospun Nanofibers for Controlled Drug Release: Recent Advances and New Perspectives. *Curr. Pharm. Des.* **2015**, *21*, 1944−1959.
(10) Muñoz-Bonilla, A.; Fernández-García, M. Polymeric Materials with Antimicrobial Activity. *Prog. Polym. Sci.* **2012**, *37*, 281−339.
(11) Xiong, M.-H.; Bao, Y.; Yang, X.-Z.; Zhu, Y.-H.; Wang, J. Delivery of Antibiotics with Polymeric Particles. *Adv. Drug Delivery Rev.* **2014**, *78*, 63−76.
(12) Chiang, W.-L.; Lin, T.-T.; Sureshbabu, R.; Chia, W.-T.; Hsiao, H.-C.; Liu, H.-Y.; Yang, C.-M.; Sung, H.-W. A Rapid Drug Release System with a NIR Light-Activated Molecular Switch for Dual-Modality Photothermal/Antibiotic Treatments of Subcutaneous Abscesses. *J. Controlled Release* **2015**, *199*, 53−62.
(13) Stebbins, N. D.; Ouimet, M. A.; Uhrich, K. E. Antibiotic-containing Polymers for Localized, Sustained Drug Delivery. *Adv. Drug Delivery Rev.* **2014**, *78*, 77−87.
(14) Ng, V. W.; Chan, J. M.; Sardon, H.; Ono, R. J.; García, J. M.; Yang, Y. Y.; Hedrick, J. L. Antimicrobial Hydrogels: A New Weapon in the Arsenal Against Multidrug-Resistant Infections. *Adv. Drug Delivery Rev.* **2014**, *78*, 46−62.
(15) Gustafson, C. T.; Boakye-Agyeman, F.; Brinkman, C. L.; Reid, J. M.; Patel, R.; Bajzer, Z.; Dadsetan, M.; Yaszemski, M. J. Controlled Delivery of Vancomycin via Charged Hydrogels. *PLoS One* **2016**, *11*, No. e0146401.
(16) Prichard, E. M.; Valentin, T.; Panilaitis, B.; Omenetto, F.; Kaplan, D. L. Antibiotic-Releasing Silk Biomaterials for Infection Prevention and Treatment. *Adv. Funct. Mater.* **2013**, *23*, 854−861.
(17) Wang, C.; Zhang, G.; Liu, G.; Hu, J.; Liu, S. Photo- and Thermo-Responsive Multicompartment Hydrogels for Synergistic Delivery of Gemcitabine and Doxorubicin. *J. Controlled Release* **2017**, *259*, 149−159.
(18) Khanal, A.; Nakashima, K. Incorporation and Release of Cloxacillin Sodium in Micelles of Poly(styrene-b-2-vinyl pyridine-b-ethylene oxide). *J. Controlled Release* **2005**, *108*, 150−160.
(19) Coll Ferrer, M. C.; Dastgheyb, S. S.; Hickok, N. J.; Eckmann, D. M.; Composto, R. J. Designing Nanogel Carriers for Antibacterial Applications. *Acta Biomater.* **2014**, *10*, 2105−2111.
(20) Forier, K.; Raemdonck, K.; De Smedt, S. C.; Demeester, J.; Coenye, T.; Braeckmans, K. Lipid and Polymer Nanoparticles for Drug Delivery to Bacterial Biofilms. *J. Controlled Release* **2014**, *190*, 607−623.
(21) Calamak, S.; Shahbazi, R.; Eroglu, I.; Gultekinoglu, M.; Ulubayram, K. An Overview of Nanofiber-based Antibacterial Drug Design. *Expert Opin. Drug Discovery* **2017**, *12*, 391−406.
(22) Frykberg, R. G.; Banks, J. Challenges in the Treatment of Chronic Wounds. *Adv. Wound Care* **2015**, *4*, 560−582.
(23) Han, G.; Ceilley, R. Chronic Wound Healing: A Review of Current Management and Treatments. *Adv. Ther.* **2017**, *34*, 599−610.
(24) Warriner, R.; Burrell, R. Infection and the Chronic Wound: A Focus on Silver. *Adv. Skin Wound Care* **2005**, *18*, 2−12.
(25) Draelos, Z. D.; Rizer, R. L.; Trookman, N. S. A Comparison of Postprocedural Wound Care Treatments: Do Antibiotic-based Ointments Improve Outcomes? *J. Am. Acad. Dermatol.* **2011**, *64*, S23−S29.
(26) Kalaoglu-Altan, O. I.; Sanyal, R.; Sanyal, A. Reactive and 'Clickable' Electrospun Polymeric Nanofibers. *Polym. Chem.* **2015**, *6*, 3372−3381.
(27) Teo, W. E.; Ramakrishna, S. A Review on Electrospinning Design and Nanofibre Assemblies. *Nanotechnology* **2006**, *17*, R89−R106.
(28) Agarwal, S.; Wendorff, J. H.; Greiner, A. Use of Electrospinning Technique for Biomedical Applications. *Polymer* **2008**, *49*, 5603−5621.
(29) Qi, R.; Guo, R.; Zheng, F.; Liu, H.; Yu, J.; Shi, X. Controlled Release and Antibacterial Activity of Antibiotic-loaded Electrospun Halloysite/Poly(lactic-co-glycolic acid) Composite Nanofibers. *Colloids Surf., B* **2013**, *110*, 148−155.
(30) Kim, K.; Luu, Y. K.; Chang, C.; Fang, D.; Hsiao, B. S.; Chu, B.; Hadjiargyrou, M. Incorporation and Controlled Release of a Hydrophilic Antibiotic using Poly(lactide-co-glycolide)-based Electrospun Nanofibrous Scaffolds. *J. Controlled Release* **2004**, *98*, 47−56.
(31) Son, Y. J.; Kim, Y.; Kim, W. J.; Jeong, S. Y.; Yoo, H. S. Antibacterial Nanofibrous Mats Composed of Eudragit for pH-Dependent Dissolution. *J. Pharm. Sci.* **2015**, *104*, 2611−2618.
(32) Demirci, S.; Celebioglu, A.; Aytac, Z.; Uyar, T. pH-Responsive Nanofibers with Controlled Drug Release Properties. *Polym. Chem.* **2014**, *5*, 2050−2056.
(33) Cheng, M.; Wang, H.; Zhang, Z.; Li, N.; Fang, X.; Xu, S. Gold Nanorod-Embedded Electrospun Fibrous Membrane as a Photothermal Therapy Platform. *ACS Appl. Mater. Interfaces* **2014**, *6*, 1569−1575.
(34) Maity, S.; Wu, W.-C.; Xu, C.; Tracy, J. B.; Gundogdu, K.; Bochinski, J. R.; Clarke, L. I. Spatial Temperature Mapping Within Polymer Nanocomposites Undergoing Ultrafast Photothermal Heating via Gold Nanorods. *Nanoscale* **2014**, *6*, 15236−15247.

DOI: 10.1021/acsami.8b14784
ACS Appl. Mater. Interfaces XXXX, XXX, XXX−XXX

(35) Chen, L.; Si, L.; Wu, F.; Chan, S. Y.; Yu, P.; Fei, B. Electrical and Mechanical Self-Healing Membrane using Gold Nanoparticles as Localized "Nano-Heaters". *J. Mater. Chem. C* **2016**, *4*, 10018−10025.
(36) Zhang, Z.; Liu, S.; Xiong, H.; Jing, X.; Xie, Z.; Chen, X.; Huang, Y. Electrospun PLA/MWCNTs Composite Nanofibers for Combined Chemo- and Photothermal Therapy. *Acta Biomater.* **2015**, *26*, 115−123.
(37) Zhang, J.; Zheng, T.; Alarçin, E.; Byambaa, B.; Guan, X.; Ding, J.; Zhang, Y. S.; Li, Z. Porous Electrospun Fibers with Self-Sealing Functionality: An Enabling Strategy for Trapping Biomacromolecules. *Small* **2017**, *13*, No. 1701949.
(38) Li, Y.; Fu, Y.; Ren, Z.; Li, X.; Mao, C.; Hana, G. Enhanced Cell Uptake of Fluorescent Drug-loaded Nanoparticles via an Implantable Photothermal Fibrous Patch for More Effective Cancer Cell Killing. *J. Mater. Chem. B* **2017**, *5*, 7504−7511.
(39) Wang, X.; Lv, F.; Li, T.; Han, Y.; Yi, Z.; Liu, M.; Chang, J.; Wu, C. Electrospun Micropatterned Nanocomposites Incorporated with Cu2S Nanoflowers for Skin Tumor Therapy and Wound Healing. *ACS Nano* **2017**, *11*, 11337−11349.
(40) Teodorescu, F.; Oz, Y.; Quéniat, G.; Abderrahmani, A.; Foulon, C.; Lecoeur, M.; Sanyal, R.; Sanyal, A.; Boukherroub, R.; Szunerits, S. Photothermally Triggered On-Demand Insulin Release from Reduced Graphene Oxide Modified Hydrogels. *J. Controlled Release* **2017**, *246*, 164−173.
(41) Qi, K.; He, J.; Wang, H.; Zhou, Y.; You, X.; Nan, N.; Shao, W.; Wang, L.; Ding, B.; Cui, S. A Highly Stretchable Nanofiber-Based Electronic Skin with Pressure-, Strain-, and Flexion-Sensitive Properties for Health and Motion Monitoring. *ACS Appl. Mater. Interfaces* **2017**, *9*, 42951−42960.
(42) Luo, Y.; Shen, H.; Fang, Y.; Cao, Y.; Huang, J.; Zhang, M.; Dai, J.; Shi, X.; Zhang, Z. Enhanced Proliferation and Osteogenic Differentiation of Mesenchymal Stem Cells on Graphene Oxide-Incorporated Electrospun Poly(lactic-co-glycolic acid) Nanofibrous Mats. *ACS Appl. Mater. Interfaces* **2015**, *7*, 6331−6339.
(43) Wang, S.-D.; Ma, Q.; Wang, K.; Chen, H.-W. Improving Antibacterial Activity and Biocompatibility of Bioinspired Electrospinning Silk Fibroin Nanofibers Modified by Graphene Oxide. *ACS Omega* **2018**, *3*, 406−413.
(44) Shao, W.; He, J.; Wang, Q.; Cui, S.; Ding, A. Biomineralized Poly(L-lactic-co-glycolic acid)/Graphene Oxide/Tussah Silk Fibroin Nanofiber Scaffolds with Multiple Orthogonal Layers Enhance Osteoblastic Differentiation of Mesenchymal Stem Cells. *ACS Biomater. Sci. Eng.* **2017**, *3*, 1370−1380.
(45) Mauro, N.; Scialabba, C.; Pitarresi, G.; Giammon, G. Enhanced Adhesion and In Situ Photothermal Ablation of Cancer Cells in Surface-Functionalized Electrospun Microfiber Scaffold with Graphene Oxide. *Int. J. Pharma* **2017**, *526*, 167−177.
(46) Chapman, T. M.; Perry, C. M. Cefepime: A Review of its Use in the Management of Hospitalized Patients with Pneumonia. *Am. J. Respir. Med.* **2003**, *2*, 75−107.
(47) Gentry, L. O.; Rodriguez-Gomez, G. Randomized Comparison of Cefepime and Ceftazidime for Treatment of Skin, Surgical Wound, and Complicated Urinary Tract Infections in Hospitalized Subjects. *Antimicrob. Agents Chemother.* **1991**, *35*, 2371−2374.
(48) Boulahneche, S.; Jijie, R.; Barras, A.; Chekin, F.; Singh, S. K.; Bouckaert, J.; Medjram, M. S.; Kurungot, S.; Boukherroub, R.; Szunerits, S. On Demand Electrochemical Release of Drugs From Porous Reduced Graphene Oxide Modified Flexible Electrodes. *J. Mater. Chem. B* **2017**, *5*, 6557−6565.
(49) Li, C.; Ye, R.; Bouckaert, J.; Zurutuza, A.; Drider, D.; Dumych, T.; Paryzhak, S.; Vovk, V.; Bilyy, R. O.; Melinte, S.; Li, M.; Boukherroub, R.; Szunerits, S. Flexible Nanoholey Patches for Antibiotic-Free Treatments of Skin Infections. *ACS Appl. Mater. Interfaces* **2017**, *9*, 36665−36674.
(50) Koening, J. L.; Angood, A. C. Raman Spectra of Poly(ethylene glycols) in Solution. *J. Polym. Sci.* **1970**, *8*, 1787−1796.
(51) Li, L.; Hsieh, Y.-L. Ultra-fine Polyelectrolyte Fibers From Electrospinning of Poly(acrylic acid). *Polymer* **2005**, *46*, 5133−5139.
(52) Wiśniewska, M.; Urban, T.; Grządka, E.; Zarko, V. I.; Gunko, V. M. Comparison of Adsorption Affinity of Polyacrylic Acid for Surfaces of Mixed Silica−Alumina. *Colloid Polym. Sci.* **2014**, *292*, 699−705.
(53) Mölne, L.; Tarkowski, A. An Experimental Model of Cutaneous Infection Induced by Superantigen-Producing *Staphylococcus aureus*. *J. Invest. Dermatol.* **2000**, *114*, 1120−1125.
(54) Dai, T.; Tegos, G. P.; Zhiyentayev, T.; Mylonakis, E.; Hamblin, M. R. Photodynamic Therapy for Methicillin-Resistant *Staphylococcus aureus* Infection in a Mouse Skin Abrasion Model. *Lasers Surg. Med.* **2010**, *42*, 38.
(55) Kugelberg, E.; Norström, T.; Petersen, T. K.; Duvold, T.; Andersson, D. I.; Hughes, D. Establishment of a Superficial Skin Infection Model in Mice by Using *Staphylococcus aureus* and *Streptococcus pyogenes*. *Antimicrob. Agents Chemother.* **2005**, *49*, 3435−3441.

DOI: 10.1021/acsami.8b14784
ACS Appl. Mater. Interfaces XXXX, XXX, XXX−XXX